View metadata, citation and similar papers at core.ac.uk

brought to you by CORE

provided by Elsevier - Publisher Connector

Biochimica et Biophysica Acta 1848 (2015) 2789–2798

Contents lists available at ScienceDirect

Biochimica et Biophysica Acta

journal homepage: www.elsevier.com/locate/bbamem

Structure and orientation of antibiotic peptide alamethicin in phospholipid bilayers as revealed by chemical shift oscillation analysis of solid state nuclear magnetic resonance and molecular dynamics simulation

Takashi Nagao [a], Daisuke Mishima [a], Namsrai Javkhlantugs [a,b], Jun Wang [a], Daisuke Ishioka [a], Kiyonobu Yokota [a], Kazushi Norisada [a], Izuru Kawamura [a], Kazuyoshi Ueda [a], Akira Naito [a,*]

[a] Graduate School of Engineering, Yokohama National University, Tokiwadai 79-5 Hodogaya-ku, Yokohama 240-8501, Japan
[b] Center for Nanoscience and Nanotechnology, School of Engineering and Applied Sciences, National University of Mongolia, Ulaanbaatar 14201, Mongolia

ARTICLE INFO

Article history:
Received 9 April 2015
Received in revised form 1 July 2015
Accepted 31 July 2015
Available online 3 August 2015

Keywords:
Antibiotic peptide
Phospholipid bilayer
Ion-channel
Chemical shift oscillation
Solid state NMR
Molecular dynamics simulation

ABSTRACT

The structure, topology and orientation of membrane-bound antibiotic alamethicin were studied using solid state nuclear magnetic resonance (NMR) spectroscopy. ^{13}C chemical shift interaction was observed in [1-^{13}C]-labeled alamethicin. The isotropic chemical shift values indicated that alamethicin forms a helical structure in the entire region. The chemical shift anisotropy of the carbonyl carbon of isotopically labeled alamethicin was also analyzed with the assumption that alamethicin molecules rotate rapidly about the bilayer normal of the phospholipid bilayers. It is considered that the adjacent peptide planes form an angle of 100° or 120° when it forms α-helix or 3_{10}-helix, respectively. These properties lead to an oscillation of the chemical shift anisotropy with respect to the phase angle of the peptide plane. Anisotropic data were acquired for the 4 and 7 sites of the N- and C-termini, respectively. The results indicated that the helical axes for the N- and C-termini were tilted 17° and 32° to the bilayer normal, respectively. The chemical shift oscillation curves indicate that the N- and C-termini form the α-helix and 3_{10}-helix, respectively. The C-terminal 3_{10}-helix of alamethicin in the bilayer was experimentally observed and the unique bending structure of alamethicin was further confirmed by measuring the internuclear distances of [1-^{13}C] and [^{15}N] doubly-labeled alamethicin. Molecular dynamics simulation of alamethicin embedded into dimyristoyl phophatidylcholine (DMPC) bilayers indicates that the helical axes for α-helical N- and 3_{10}-helical C-termini are tilted 12° and 32° to the bilayer normal, respectively, which is in good agreement with the solid state NMR results.

© 2015 Elsevier B.V. All rights reserved.

1. Introduction

Alamethicin is an antibiotic peptide from *Trichoderma viride* that consists of 20 amino acid residues [1]. One of the major amino acid sequences is Ac-Aib-Pro-Aib-Ala-Aib-Ala-Gln-Aib-Val-Aib-Gly-Leu-Aib-Pro-Val-Aib-Aib-Glu-Gln-Phol in which 8 or 9 α-aminoisobutyric acids (Aib) are included. In addition, the N-terminus is acetylated and the C-terminus is terminated as L-phenylalaninol (Pheol) [2,3]. Alamethicin consists of heterogeneous mixture of which the major constituents which were distinctively detected by thin-layer chromatography (TLC), and named as alamethicin F30 and F50 with molar ratios of 0.85 and 0.12, respectively. Alamethicin F30 and F50 contain Glu18 and Gln18, respectively [4].

Alamethicin is known to exhibit voltage dependent ion channel activity in membrane environments [5]. Alamethicin has a high affinity for lipid bilayers, therefore, alamethicin binds to the surface of lipid bilayers and can be inserted into the membrane. The orientation of alamethicin in a lipid bilayer is dependent on the peptide/lipid (P/L) molar ratios [6,7], the type of lipid bilayers, and the membrane potentials [8]. Various channel models have been proposed to determine the ion channel activity, such as the barrel–stave model [9]. Alamethicin channels are formed by parallel bundles of the transmembrane helical monomers surrounding a central water-filled pore, and are composed of 3–12 alamethicin molecules [10,11]. The ion channel activity of alamethicin makes it a suitable model to investigate voltage dependent ion channel proteins [12,13].

X-ray crystallographic analysis indicates that alamethicin takes a helical structure where the kink position is Pro14, and the N- and C-termini take the α-helix and 3_{10}-helix structures, respectively [9]. Solution nuclear magnetic resonance (NMR) studies show that the N-terminus forms an α-helix and the C-terminus takes a variety of helix structure depending on the conditions [14–17]. In addition, circular dichroism, infrared, and Raman spectroscopies show that alamethicin

* Corresponding author.
E-mail address: naito@ynu.ac.jp (A. Naito).

http://dx.doi.org/10.1016/j.bbamem.2015.07.019
0005-2736/© 2015 Elsevier B.V. All rights reserved.

takes a variety of helix structure in the solvents [18–21]. Furthermore, it is realized that poly-Aib takes 3_{10}-helix [22]; therefore, it is of interest to determine if the C-terminus of alamethicin may take the 3_{10}-helix structure in a membrane environment.

The conformation and orientation of membrane-bound alamethicin have been studied using solid-state NMR spectroscopy measurements with dimyristoyl phosphatidylcholine (DMPC)/dihexanoyl phosphatidylcholine (DHPC) mixed lipid bilayer systems (bicelle). ^{13}C chemical shifts of isotopically labeled alamethicin indicated that alamethicin forms an α-helical structure in a lipid bilayer and is oriented along the bilayer normal. The chemical shift anisotropy was substantially reduced by rotation of the alamethicin helix about the bilayer normal [23].

Two-dimensional separated local field ^{15}N NMR spectra were obtained using the same motional model of alamethicin where the peptides rotate about the bilayer normal. The results reveal a ^{15}N-^{1}H dipolar splitting of 17 kHz, which indicates that the N–H bond tilts 24° with respect to B_0. This angle was evaluated by assuming that the maximum dipolar splitting is 22.6 kHz and the N–H bond length is 1.024 Å [24]. These data are consistent with an α-helical conformation inserted along the bilayer normal [24].

The conformation of alamethicin in mechanically oriented phospholipid bilayers has been further studied using ^{15}N solid-state NMR in combination with molecular modeling and molecular dynamics (MD) simulations. ^{15}N-labeled variants at different positions of alamethicin along with three of Aib residues replaced by Ala were examined. From the anisotropic ^{15}N chemical shift and ^{1}H-^{15}N dipolar couplings determined for alamethicin with ^{15}N-labeling on the Ala6, Val9, and Val15 residues incorporated into phospholipid bilayers with a peptide-to-lipid molar ratio of 1:8, it was determined that alamethicin has a largely linear α-helical structure that spans the membrane with the molecular axis tilted by 10–20° relative to the bilayer normal. In particular, the compatibility with a straight α-helix was tilted by 17° and a slightly kinked molecular dynamics structure was tilted by 11° relative to the bilayer normal [25]. Measurement of the orientation-dependent ^{1}H–^{15}N dipole-dipole coupling, ^{15}N anisotropic chemical shift, and ^{2}H quadrupole coupling parameters for a single residue, combined with analysis of anisotropic interaction for the Aib8 residue provides detailed information regarding helix-tilt angle, wobbling and oscillatory rotation around the helix axis in the membrane bound state of alamethicin [26].

Alamethicin samples were uniformly labeled with ^{15}N and reconstituted into oriented palmitoyl oleoylphosphatidylcholine (POPC) and DMPC membranes. Proton–decoupled ^{15}N solid-state spectra showed that alamethicin adopts a transmembrane orientation with reconstitution into the POPC oriented membrane [27]. Two-dimensional ^{15}N chemical shift ^{1}H–^{15}N dipolar coupling solid-state NMR correlation spectroscopy (PISEMA) suggests that alamethicin in the transmembrane configuration adopts a mixed $\alpha/3_{10}$ helical structure with a tilt angle of 8.9° with respect to the bilayer normal [28].

Although, many studies show that alamethicin forms a transmembrane helix in a membrane environment, it is yet to be clarified whether the helix is bent or straight, which part of alamethicin forms the 3_{10}-helix, and whether alamethicin molecules associate with each other in the membrane environment.

We have previously reported that anisotropic chemical shift interaction in a peptide bound to membrane may exhibit chemical shift oscillation [29]. This chemical shift oscillation enables evaluation of the tilt angle of the helix and the kink angle between the two existing helices in the membrane bound peptide, as long as they rotate rapidly about the bilayer normal without using oriented membranes. From the chemical shift oscillation analysis, tilt angles with respect to the bilayer normal and phase angle of the peptides around the helical axis were determined for a variety of membrane bound peptides, such as melittin [30,31], dynorphin [32], bombolitin-II [33] and lactoferrampin [34]. In addition, it is possible to determine the existence of different types of helices within the molecule as well as the topology of the helices as was preliminarily demonstrated for alamethicin embedded in a membrane [29].

MD simulations of peptides in the membrane environment have been useful tools to investigate dynamic structure, topology and orientation with respective to membrane normal [8,35–38] and compared with those determined by solid-state NMR [25,26,33,34]. Furthermore, MD simulations provided the insight into peptide–peptide and peptide–lipid interaction networks [39].

In this study, we attempt to analyze 4 labeled sites in the N-terminus and 7 labeled sites for the C-terminus including Aib residues, which have not been labeled in the previous study. Chemical shift values for individually labeled carbonyl carbon nuclei are determined. A number of ^{13}C–^{15}N internuclear distances are also determined in order to determine the topology of alamethicin bound to membrane. The combination of chemical shift oscillation and inter-nuclear distance measurements allows to evaluation of the detailed structure, topology and orientation of alamethicin in the membrane bound state, which has not been determined in previous solid state NMR studies. MD simulations are performed to justify the accurately determined NMR structure of alamethicin in membrane environments.

2. Materials and methods

2.1. Sample preparation

The F50 amino acid sequence of alamethicin was adopted in this study and the C-terminal was methyl esterified. This modification made it possible to synthesize a number of labeled peptides with high yields. Although the C-terminus of alamethicin is not methyl ester but amino alcohol, it has been reported that this modification does not significantly affect the activity of alamethicin [24]. The sequence of alamethicin used in this study is as follows

Ac-Aib-Pro-Aib-Ala-Aib-Ala-Gln-Aib-Val-Aib-Gly-Leu-Aib-Pro-Val-Aib-Aib-Gln-Gln-PheOCH$_3$.

Eleven types of singly labeled [1-^{13}C]Ala6, Gln7, Val9, Aib10, Gly11, Leu12, Aib13, Val15, Aib16, Aib17, or Gln18-alamethicin molecules were synthesized using fluoreylmethyloxycarbonyl (Fmoc) chemistry and solid phase methods. 9-Fluorerylmethhoxycarbonyl (Fmoc)-labeled amino acids were synthesized from 9-fluorenyl N-succinimidyl carbonate (Fmoc Osu) and isotoropically labeled amino acids, following a method by Paquet [40]. A standard protocol of peptide synthesis using peptide synthesizer is described in the previous literature [41], Instead of using 1-hydroxybenzotriazole (HOBt), Fmoc-amino acids were activated using 1-[bis(dimethylamino)methylene]-1H-1,2,3-triazole[4,5-b]pyridium 3-oxid hexafluorophosphate (HATU)/dimethylformamide (DMF) in the presence of N,N-diisopropylethylamine (DIPEA), followed by amino acid coupling with stepwise cycles, because Aib has bulky sidechain to reduce the coupling activity. The synthesized peptide was treated with acetic anhydride to acetylate the N-terminus and dissolved in methanol in the presence of trifluoroacetic acid (TFA) to form the methyl ester at the C-terminus. This alamethicin analogue was purified using a Waters 600E high performance liquid chromatography (HPLC) system equipped with a Bondaphase C_{18} reversed phase column. Fifty milligrams of ^{13}C labeled alamethicins and dimyristoyl phosphatidylcholine (DMPC), with a alamethicin-to-DMPC molar ratio of 1:10, was dissolved in methanol, and solvent was subsequently evapolated *in vacuo*, followed by hydration with 600 μl of Tris buffer (20 mM Tris, 100 mM NaCl, and pH 7.5). A freeze–thaw cycle was repeated 10 times, followed by centrifugation to concentrate the bilayers. Finally, the total volume was adjusted to 300 μl containing 50 mg of lipid and alamethicin. The lipid bilayers were filled in zirconia or glass sample tube for magic angle spinning (MAS) or static NMR measurements, respectively.

2.2. NMR measurements

^{13}C NMR measurements were performed on a Chemagnetics CMX infinity-400 NMR spectrometer operated at the ^{13}C and ^{1}H resonance frequencies of 100.11 and 398.89 MHz, respectively. For ^{13}C direct excitation with high power proton decoupling (DD) NMR experiments of the hydrated alamethicin-DMPC membrane dispersions, a 5.0 μs of excitation pulse of 90° was used under a high power proton decoupling amplitude of 66 kHz, with a repetition time of 4 s. ^{13}C DD NMR spectra were acquired under static and magic angle spinning (MAS) (spinning frequency of 2 kHz) conditions. To determine the principal values of the ^{13}C chemical shift tensors of the carbonyl carbons, ^{13}C NMR spectra of the lyophilized powder samples were measured at 20 °C using cross polarization and MAS (CP–MAS) with a contact time of 1 ms and a spinning frequency of 2 kHz. The principal values were determined by comparing the sideband patterns obtained in the CP–MAS experiment with the simulated ^{13}C NMR spectra. ^{13}C chemical shift values were externally referenced with respect to 176.03 ppm for the carboxyl carbon of glycine from that for tetramethylsilane (TMS).

^{13}C Rotational-echo double-resonance (REDOR) spectra were measured using an xy-4 irradiation pulse to compensate the errors of flip angle, off resonance effect, and fluctuation of the rf field for ^{13}C nuclei [42]. The π pulse lengths for ^{13}C and ^{15}N nuclei were 13.0 and 13.9 μs, respectively. The proton decoupling amplitude was 70 kHz. The rotor frequency was controlled to 4000 ± 2 Hz. REDOR and full echo spectra were recorded at various NcTr values from 5 to 25 ms, where Nc and Tr are the number of rotor cycles and the rotor period, respectively. The normalized REDOR differences were evaluated as follows

$$\Delta S/S_0 = (S_{full} - S_{REDOR})/S_{full}, \tag{1}$$

where, S_{REDOR} and S_{full} are the peak intensities of the REDOR and full echo spectra, respectively. These REDOR differences were plotted against the NcTr values to fit the theoretically obtained curves by considering the π-pulse length to determine the ^{13}C–^{15}N internuclear distances [43].

2.3. Analysis of dynamic structure of helical peptide bound to lipid bilayer based on chemical shift oscillation

In the case of helical peptide bound to a lipid bilayer, it has been established that the peptide rotates about the bilayer normal [30,31]. In that dynamical state, an axially symmetric powder pattern characterized by $\delta_{//}$ and $\delta_{\perp}$, is observed and the chemical shift anisotropy $\Delta\delta = \delta_{//} - \delta_{\perp}$, for carbonyl carbon can be expressed as

$$(\Delta\delta) = \frac{3}{2}\sin^2\varsigma\left(\delta_{11}\cos^2\gamma_i + \delta_{33}\sin^2\gamma_i - \delta_{22}\right) + (\overline{\Delta\delta})_{\varsigma=0}, \tag{2}$$

$$(\overline{\Delta\delta})_{\varsigma=0} = \delta_{22} - \frac{\delta_{11}+\delta_{33}}{2}, \tag{3}$$

where, δ_{11}, δ_{22} and δ_{33} indicate the principal values of the chemical shift tensors for the rigid carbonyl carbon nucleus, ζ is the tilt angle of the helix axis with respect to the bilayer normal, and γ_i is the phase angle of the peptide plane of the i-th residue about the helical axis (Fig. S1) [31]. Eq. (2) indicates that the chemical shift anisotropy Δδ, will behave as an oscillation, which is referred to as a chemical shift oscillation with an amplitude of $\frac{3}{2}\sin^2\varsigma$ and the phase angle of γ_i. One cycle of the α-helix consists of 3.6 residues; therefore, $\gamma_{i+1} - \gamma_i = -100°$. On the other hand, one cycle of the 3_{10}-helix consists of 3 residues, so that $\gamma_{i+1} - \gamma_i = -120°$. Chemical shift anisotropies, $\Delta\delta_{obs}$, can be observed in a variety of labeled samples and they provide plots of chemical shift anisotropy against γ, which indicate the chemical shift oscillation patterns. It is important to note that one cycle of the chemical shift oscillation corresponds to 1.8 (180°) and 1.5 (180°) residues and adjacent peptide planes make angles of 100° and 120° for the α- and 3_{10}-helices, respectively, as shown in Eq. (2). Thus, the $\Delta\delta_{obs}$ values can be used to evaluate root mean square deviation (RMSD) with the calculated values, $\Delta\delta_{calc}$ as is given by

$$RMSD = \sqrt{\sum_{i=1}^{N}\left[(\Delta\delta_{obs})_i - (\Delta\delta_{calc})_i\right]^2/N}. \tag{4}$$

In this work, chemical shift values were obtained for N number of residues and the RMSD values were calculated with experimentally obtained δ_{11}, δ_{22}, and δ_{33} values using Eq. (4) with various ζ and γ values. Finally, the most probable structure can be evaluated by searching the minimum value of RMSD. It is also possible to distinguish the α-helix and 3_{10}-helix by considering the degree of one cycle in the chemical shift oscillation pattern.

2.4. Computational procedure

MD simulation was performed using CHARMM software [44] with an all-atom force field [45,46] to investigate the dynamic structure and orientation of the alamethicin peptide in the DMPC membrane bilayer. The α-helical conformation of alamethicin peptide was constructed as an initial structure for the simulation using the same procedure as previously reported [34,35]. The residues at the N- and C-terminals of the alamethicin peptide were capped with acetyl (Ac-) and methyl ($-CH_3$) groups, respectively. The alamethicin peptide was placed in the membrane with the principal axis of the backbone atoms parallel to the membrane normal. The membrane builder module [47] of CHARMM-GUI [48] was used to build the initial conformation for MD simulation with a concentration of 100 mM NaCl. The final model includes the alamethicin peptide, 96 lipid and 2717 water molecules, 6 sodium and 6 chloride ions: and the total number of atoms in the system is 19,783. The isobaric–isothermal (NPT) ensemble was conducted with 1 fs time steps for 40 ns. The details of the calculation procedure are the same as used in our previous simulations [34,35].

3. Results and discussion

3.1. ^{13}C NMR spectra of carbonyl carbons of alamethicin bound to DMPC bilayers

Fig. 1 shows ^{13}C DD–MAS NMR spectra for hydrated [1-^{13}C] labeled alamethicin–DMPC bilayer systems in the liquid crystalline phase at 40 °C. Isotropic chemical shifts of the carbonyl carbons in a variety of amino acid residues are evaluated and summarized in Table 1. All the positions showed that alamethicin takes a helical structure in the entire region as determined from the conformation dependent chemical shift values [49,50]. The δ_{iso} values for [1-^{13}C]Val9 and [1-^{13}C]Aib13 deviated from those of the helix structure, and hence the vicinities of Val9 and Aib13 also deviated from the helical structure. It was not possible to distinguish an α-helix from a 3_{10}-helix using the conformation dependent chemical shift values, although X-ray data indicated that the N- and C-terminal parts of alamethicin form the α-helix and 3_{10}-helix structures, respectively [9].

Fig. 2 shows powder ^{13}C DD NMR spectra for hydrated alamethicin–DMPC bilayer system in the liquid crystalline phase at 40 °C under the static condition. The powder spectra clearly show the axially symmetric shape, which indicates that alamethicin molecules rotate about the unique axis in the liquid crystalline phase. It is well established that the rotation axis of alamethicin is the bilayer normal, the same as that demonstrated for melittin-bilayer systems [30]. The $\delta_{\perp}$, $\delta_{//}$, and Δδ values of ^{13}C carbonyl carbons for [1-^{13}C]Ala6, [1-^{13}C]Gln7, [1-^{13}C]Val9, [1-^{13}C]Aib10, [1-^{13}C]Gly11, [1-^{13}C]Leu12, [1-^{13}C]Aib13, [1-^{13}C]Val15, [1-^{13}C]Aib16, [1-^{13}C]Aib17, and [1-^{13}C]Gln18 were determined

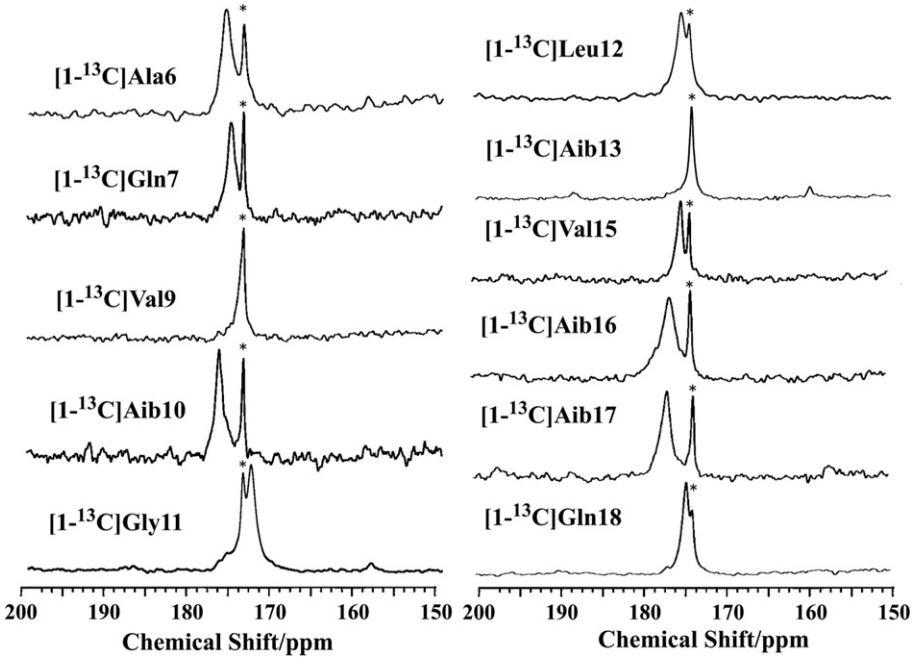

Fig. 1. ^{13}C DD MAS NMR spectra for singly labeled [1-^{13}C]Ala6, [1-^{13}C]Gln7, [1-^{13}C]Val9, [1-^{13}C]Aib10, [1-^{13}C]Gly11, [1-^{13}C]Leu12, [1-^{13}C]Aib13, [1-^{13}C]Val15, [1-^{13}C]Aib16, [1-^{13}C]Aib17 and [1-^{13}C]Gln18–alamethicin molecules embedded in DMPC lipid bilayers at 40 °C. Asterisks (*) indicate the ^{13}C NMR signals for the carbonyl carbon of DMPC.

in the ^{13}C NMR powder spectra (Fig. 2) and summarized in Table 1. These values were justified by comparing them with the respective simulated spectra (Fig. S2). It was also noted that the anisotropies are varied to a large extent in an oscillatory manner among the individual residues. This change of chemical shift anisotropy indicates that the helical axis of alamethicin may largely tilt toward the bilayer normal as indicated in Eq. (2). Furthermore, the change of Δδ for the N-terminal helix is smaller than that for the C-terminal helix, as summarized in Table 1. It is evident that two helices exist and the C-terminal helical axis has a larger tilt angle with respect to the bilayer normal than that of the N-terminal helix. A detailed analysis of the Δδ variation is given later.

Anisotropic chemical shift pattern for individual residues of the rigid state appeared as side band patterns in the lyophilized alamethicin-DMPC bilayer systems under the slow MAS condition with a 2 kHz spinning rate as shown in Fig. 3. The principal values of the chemical shift tensors, δ_{11}, δ_{22} and δ_{33}, for the individual residues were determined by comparison of the experimental side-band intensity patterns (Fig. 3) with those of simulated side band intensity patterns (Fig. S3). The side band intensity patterns are slightly different among the residues and the principal values of the chemical shift tensors are summarized in Table 1.

Table 1
^{13}C chemical shift values (ppm) for [1-^{13}C]–alamethicin bound to DMPC lipid bilayers.

	$d_{//}$	$d_{\perp}$	Δδ	δ_{11}	δ_{22}	δ_{33}	δ_{iso}	Structure
Ala6	182.8	173.6	9.2	245	191	94	176.7	Helix
Gln7	191.6	167.9	23.8	247	186	95	175.8	Helix
Val9	182.1	169.5	12.6	245	184	94	173.7	Helix*
Aib10	180.5	176.4	4.1	251	185	98	177.8	Helix
Gly11	188.4	164.4	24.0	247	175	96	172.3	Helix
Leu12	173.0	176.1	−3.1	240	193	93	175.1	Helix
Aib13	201.5	159.6	41.9	245	179	97	173.6	Helix*
Val15	188.2	168.6	19.5	243	186	97	175.2	Helix
Aib16	163.0	182.7	−19.7	246	185	98	176.1	Helix
Aib17	202.1	164.2	37.9	242	188	101	176.8	Helix
Gln18	186.1	169.0	17.1	248	181	96	174.7	Helix

* Chemical shift values deviate from the typical value for the helix structure.

3.2. ^{13}C REDOR spectra for alamethicin bound to lyophilized lipid bilayers

The internuclear ^{13}C-^{15}N distances of [1-^{13}C]Gln7-[^{15}N]Gly11, [1-^{13}C]Gly11-[^{15}N]Pro14, [1-^{13}C]Aib10-[^{15}N]Val15, and [1-^{13}C]Val15-[^{15}N]Gln19 were measured using the REDOR method to determine the three dimensional structure of alamethicin bound to lipid bilayers in the lyophilized sample, which is postulated to be the immobile state. Fig. 4 shows the, $\Delta S/S_0$ values plotted against NcTr values for [1-^{13}C]Gln7-[^{15}N]Gly11 (A), [1-^{13}C]Gly11-[^{15}N]Pro14 (D), [1-^{13}C]Val15-[^{15}N]Gln19 (B), and [1-^{13}C]Aib10-[^{15}N]Val15 (C), where Nc is the number of rotor cycles and Tr is the rotor cycle period. Inspecting of the best fit plots to the experimentally obtained values yielded distances of 4.3 ± 0.2, 4.4 ± 0.1, 4.6 ± 0.5, 6.5 ± 0.7 Å for [1-^{13}C]Gln7-[^{15}N]Gly11, [1-^{13}C]Gly11-[^{15}N]Pro14, [1-^{13}C]Val15-[^{15}N]Gln19, and [1-^{13}C]Aib10-[^{15}N]Val15, respectively (Table 2). The distance of 4.3 Å for [1-^{13}C]Gln7-[^{15}N]Gly11 indicate that Gln7 and Gly11 form hydrogen bonds in the α-helix structure, because residues i and i + 4 form hydrogen bonds. On the other hand, the distance of 4.4 Å for [1-^{13}C]Gly11-[^{15}N]Pro14 indicates that Gly11 and Pro14 as short as forming hydrogen bonds in the 3_{10}-helix structure, because residues between i and i + 3 form hydrogen bonds, although Pro14 may not form hydrogen bonds. This result indicates that the N-terminus of alamethicin forms an α-helix, while the C-terminus of alamethicin forms a 3_{10}-helix. This result also indicates that the bending of helix axis starts from the Gly11 residue, and the α-helix also changes to a 3_{10}-helix at the position of Gly11. It is also expected that the distances for [1-^{13}C]Gly11-[^{15}N]Pro14 and [1-^{13}C]Aib10-[^{15}N]Val15 may provide information regarding the bending angle between the N- and C-terminal helices.

3.3. Analysis of chemical oscillation pattern to elucidate the structure

It is expected that the N-terminal part of alamethicin forms an α-helix in the lipid bilayers, therefore, RMSD values were calculated for various ζ and γ values changed by 1° steps using the chemical shift data for Ala6, Gln7, Val9, and Aib10. Contour maps of the RMSD values are shown in Fig. 5A and B, which correspond to the α-helix and 3_{10}-helix for the N-terminus, respectively. The minimum values appeared clearly in both cases, with 2.8 and 6.4 for α-helix and 3_{10}-helix,

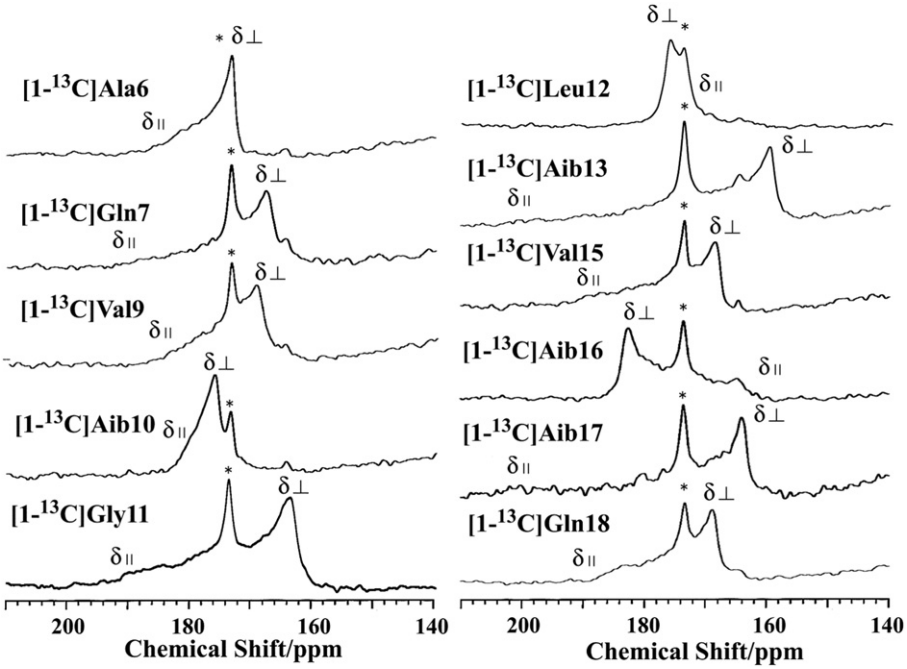

Fig. 2. ^{13}C DD NMR spectra for singly labeled [1-^{13}C]Ala6, [1-^{13}C]Gln7, [1-^{13}C]Val9, [1-^{13}C]Aib10, [1-^{13}C]Gly11, [1-^{13}C]Leu12, [1-^{13}C]Aib13, [1-^{13}C]Val15, [1-^{13}C]Aib16, [1-^{13}C]Aib17 and [1-^{13}C]Gln18–alamethicin molecules embedded in DMPC lipid bilayers at 40 °C. Asterisks (*) indicate the ^{13}C NMR signals of carbonyl carbon for the DMPC. $\delta_\perp$ and $\delta_{//}$ indicate the perpendicular and parallel components of the axially symmetric powder patterns.

respectively, which indicates that α-helix structure is more probable than the 3_{10}-helix for the N-terminus of alamethicin. The angles of ζ and γ were evaluated to be 17° and 89° (with respect to Ala6), respectively. Similarly, the minimum RMSD values for the C-terminus part were calculated using the Val15, Aib16, Aib17 and Gln18 amino acid residues, as shown in Fig. 5C and D. The minimum RMSD values were 13.7 and 4.7 for the α-helix and 3_{10}-helix, for the C-terminus of alamethicin, respectively. This result clearly indicates that the 3_{10}-helix is the more probable structure for the C-terminus, as revealed by the chemical shift oscillation patterns of alamethicin. The ζ and γ values for the C-terminal 3_{10}-helix were 32° and 37° (with respect to Val15), respectively.

3.4. Analysis of the chemical shift patterns for alamethicin bound to lipid bilayers

To elucidate a more detailed structure of alamethicin bound to lipid bilayers, chemical shift oscillation patterns, $\Delta\delta_r = (\Delta\delta) - (\overline{\Delta\delta})_{\xi=0}$ vs γ, were plotted for the most reliable ζ and γ values for the α-helix of the N-terminus and the 3_{10}-helix of the C-terminus, as shown in Fig. 6. Two different helices with different tilt angles are connected around Aib10 and Gly11 with a tilt angle of $\zeta = 17°$ for the N-terminal helix and $\zeta = 32°$ for the C-terminal helix to the bilayer normal, respectively. The amplitude of oscillation for the C-terminal helix is larger than that for the N-terminal helix, which indicates that the tilt angle for the C-

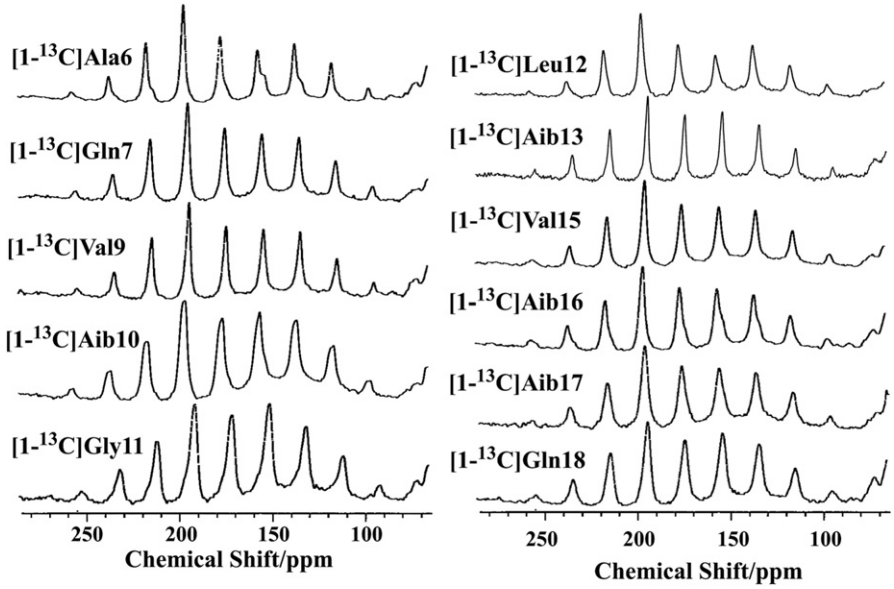

Fig. 3. ^{13}C CP MAS NMR spectra for lyophilized singly labeled [1-^{13}C]Ala6, [1-^{13}C]Gln7, [1-^{13}C]Val9, [1-^{13}C]Aib10, [1-^{13}C]Gly11, [1-^{13}C]Leu12, [1-^{13}C]Aib13, [1-^{13}C]Val15, [1-^{13}C]Aib16, [1-^{13}C]Aib17 and [1-^{13}C]Gln18–alamethicin molecules embedded in DMPC lipid bilayers at 20 °C using spinning frequency of 2 kHz.

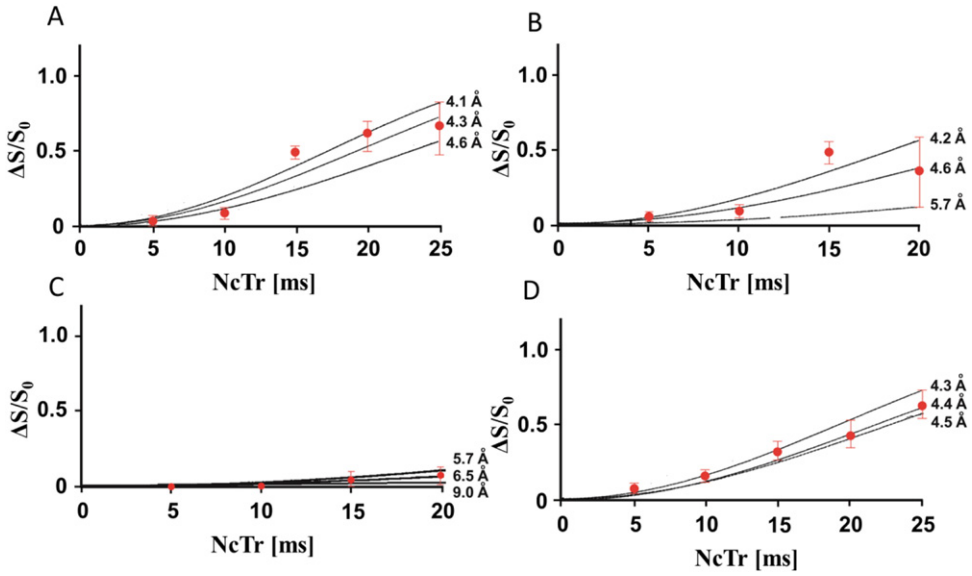

Fig. 4. Plot of $\Delta S/S_0$ values against NcTr time (ms) for ^{13}C–^{15}N distances for (A) [1-^{13}C]Gln7–[^{15}N]Gly11, (B) [1-^{13}C]Val15–[^{15}N]Gln19, (C) [1-^{13}C]Aib10–[^{15}N]Val15, and (D) [1-^{13}C]Gly11–[^{15}N]Pro14. Solid lines are calculated for the distances indicated at the right.

terminal helix (32°) is significantly larger than that of the N-terminal helix (17°). The chemical shift anisotropies of Leu12 and Aib13 show significant deviation from the best fit chemical oscillation pattern for the 3_{10}-helix of the C-terminus. Thus, it is expected that residues 12–14 are slightly distorted from the structure of the 3_{10}-helix compared with the 15–18 residue part of the C-terminus, in which Aib16 and Aib17 are successively connected. From the chemical shift oscillation curve, it is estimated that one cycle of the N-terminus is 1.8 residues and $\gamma_1 - \gamma_{i+1}$ is 100°, which indicate that one cycle of the α-helix contain 3.6 residues, while one cycle of the C-terminus is estimated to be 1.5 residues and $\gamma_1 - \gamma_{i+1}$ is 120°, which indicate that one cycle of the 3_{10}-helix contains 3 residues. This oscillation pattern clearly demonstrates that the N- and C-termini of alamethicin in the membrane environment form α- and 3_{10}-helices, respectively, and the helix axis bends at around Gly11 and changes from an α- to a 3_{10}-helix, although the 3_{10}-helix around Gly11–Pro14 deviates from the typical 3_{10}-helix structure.

3.5. Topological analysis using energy minimization based on tilt and phase angles, and internuclear distances

From the chemical oscillation analysis, the tilt angles of N- and C-termini were determined to be 17° and 32°, respectively, and the N- and C-termini were identified as α- and 3_{10}-helices, respectively. The respective phase angles of the N- and C-terminal helices are 89° with respect to Ala6, and 37° with respect toVal15. Although the tilt and phase angles were determined, possible topologies of alamethicin with two helices ($\zeta_C = \pm 32°$, $\gamma_C = +37°$ or $-143°$) and ($\zeta_N = \pm 17°$, $\gamma_N = +89°$ or $-91°$) are 16 different combinations, as shown in Figs. S4 and S5. To select one of these combinations for the topologies, energy minimization processes were performed based on the constraints of the experimental data.

Table 2
Distances between carbonyl carbon and amide nitrogen atoms in the helical backbone for some selected residues, labeled 1-^{13}C and ^{15}N atoms in the REDOR solid-state NMR.

Atoms		Distance [Å]	
1-^{13}C	^{15}N	Experimental	Simulation
Gln7	Gly11	4.3 ± 0.2	4.2
Aib10	Val15	6.5 ± 0.7	7.2
Gly11	Pro14	4.4 ± 0.1	5.2
Val15	Gln19	4.6 ± 0.5	4.4

The structure was generated by energy minimization, using the Amber99 force field and algorithms contained in MOE (Molecular Operating Environment, ver. 2007.09; Chemical Computing Group Inc.), starting from an initial peptide conformation generated manually with the protein building function of MOE. For residues 1–10 and 12–20, standard α-helix and 3_{10}-helix dihedral angles were taken, respectively.

The distance constraints from the angle of the main-chain determined from REDOR measurements were 4.3 ± 0.2, 4.4 ± 0.1, 4.6 ± 0.5 and 6.5 ± 0.7 Å for carbonyl of Gln7-amide of Gly11, carbonyl of Gly11-amide of Pro14, carbonyl of Val15-amide of Gln19 and carbonyl of Aib10-amide of Val15, respectively. The two helical bending angle constraints for the 1–10, 10–12 and 12–20 residues is 162–169°. Dihedral angle constraints of 1–10 and 12–20 are ±1.5°, respectively. The structure of alamethicin determined by this calculation is shown in Fig. S6. The calculated results indicate that ($\zeta_N = +17°$, $\gamma_N = -91°$) and ($\zeta_C = +32°$ and $\gamma_C = +37°$), and the structure has a topology with alamethicin bound to the lipid bilayers, as shown in Fig. 7. Thus, the N-terminal helix forms an α-helix with a tilt angle of 17° to the bilayer normal and the C-terminal helix forms a 3_{10}-helix with a tilt angle of 32° to the bilayer normal. The bending angle of the two helices was determined to be 165°. The α-helix structure (Aib1–Gly11) in the N-terminus consequently changes to a 3_{10}-helix structure in the C-terminus without taking a loop structure. However, the experimental chemical shift anisotropies of Leu12 and Aib13 significantly deviated from the best fit chemical shift oscillation curve. This result indicates that the 3_{10}-helix is not formed over the entire region of the C-terminus, but deviates from the 3_{10}-helix structure in the region from Leu12–Pro14 and again forms the 3_{10}-helix in the region of Val15–Gln18.

3.6. MD simulation of alamethicin bound to DMPC bilayers

In the previous MD simulation study on alamethicin, voltage-dependent insertion of alamethicin at phospholipid bilayer was investigated [8]. The results indicated that fluctuation of turn, 3_{10}- and α-helix structures occurred, but overall, the peptide lost all of the structures in 10 ns in alamethicin/POPC bilayer system. MD simulations of alamethicin in membrane environment were performed and compared with the structures determined by solid and liquid state NMR data [25,26,51]. The results of solid-state NMR indicated that straight α-helix structure was tilted by 10–20° with respect to the bilayer normal [25]. The results of MD structure suggested that the α-helix was tilted by

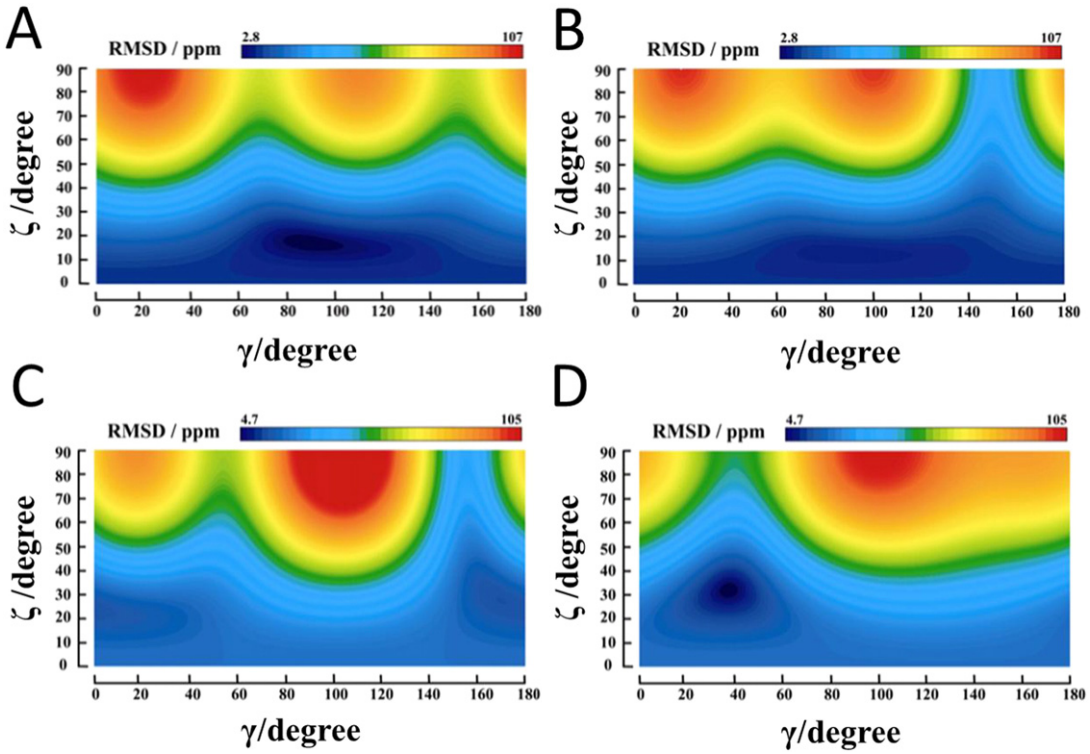

Fig. 5. Contour maps of the RMSD values for (A) the N-terminal α-helix and (B) 3_{10}-helix and (C) the C-terminal α-helix and (D) 3_{10}-helix. The minimum RMSD values for the α-helix (A) is 2.8 with $\zeta = 17°$ and $\gamma = 89°$ (with respect to Ala6), and that for the 3_{10}-helix (B) is 6.4 with $\zeta = 13°$ and $\gamma = 87°$ (with respect to Ala6). The minimum RMSD values for the α-helix (C) is 13.7 with $\zeta = 27°$ and $\gamma = 170°$ (with respect to Val15), and that for the 3_{10}-helix (D) is 4.7 with $\zeta = 32°$ and $\gamma = 37°$ (with respect to Val15).

17° and a kinked structure was tilted by 11° with respect to the bilayer normal [25]. However, the previous MD work in the solvent environment could not compare the structure, topology and orientation with those accurately determined by solid state NMR, although range of tilting angle and possibility of 3_{10}-helix are suggested reasonably.

In this present work, an MD simulation was performed to elucidate the dynamic behavior of alamethicin in the membrane environment and compared with the presently determined accurate structure, topology and orientation in the membrane environment. Fig. 8 shows a snapshot of the MD simulation after 40 ns. The helical axes of the N- and C-terminal sides are shown to tilt with different angles after the MD simulation, although the initial orientation of alamethicin was set parallel to the membrane normal. The C-terminal side of the alamethicin peptide appears more tilted than the N-terminal side. To

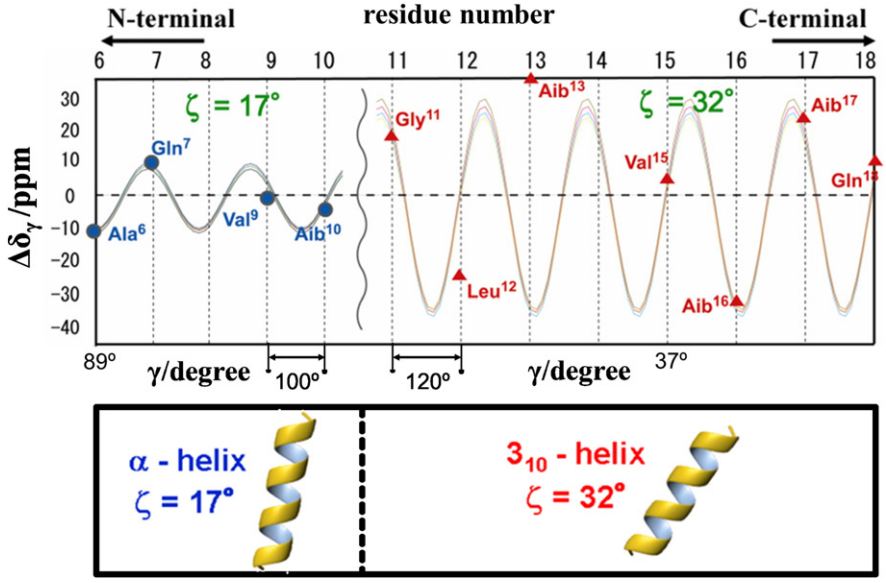

Fig. 6. Chemical shift oscillation patterns, $\Delta\delta_\gamma = (\Delta\delta) - (\overline{\Delta\delta})_{\xi=0}$ vs γ, for the N-terminal α-helix and C-terminal 3_{10}-helix with $\zeta = 17°$ and 32°, respectively. Δδ values for Ala6, Gln7, Val9 and Aib10 fit the oscillation curves for the α-helix with a tilt angle of 17°, and those for Gly11, Leu12, Aib13, Val15, Aib16, Aib17 and Gln18 fit the oscillation curve for the 3_{10}-helix with a tilt angle of 32°.

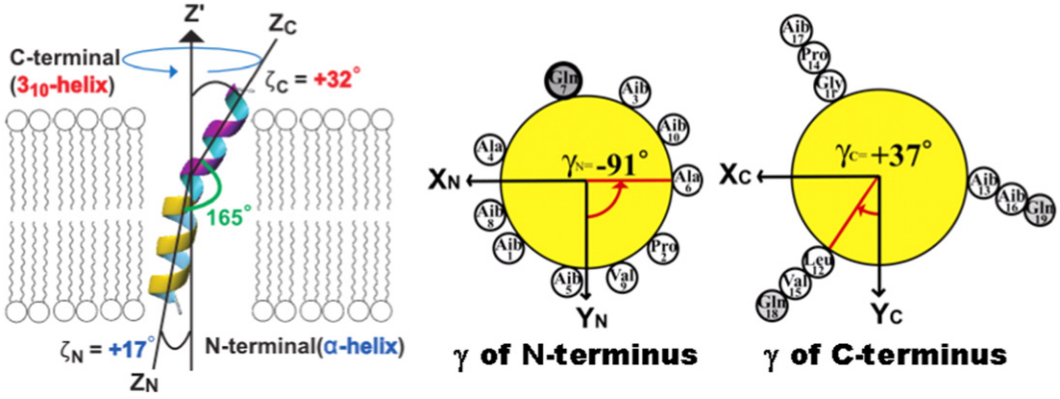

Fig. 7. Secondary structure, orientation and topology of alamethicin bound to lipid bilayers. The N-terminal α-helix tilted +17° to the bilayer normal and the C-terminal 3_{10}-helix is tilted +32° to the bilayer normal and the bending angle is 165°. Phase angles of Ala6 for the N-terminal α-helix and Val15 for the C-terminal 3_{10}-helix are −91° and +37°, respectively.

investigate the tilting behavior of these two sides more precisely, time courses of the tilt angles for Ala6 and Val15 were analyzed and the results are shown in Fig. 9 (top). The tilt angle ζ, were calculated from the angle between the direction of the C═O and the membrane normal. The angles fluctuate from the initial value but gradually approach the equilibrium state after approximately 30 ns. The tilt angles during the last 10 ns of the MD simulation were averaged and are shown in Fig. 9 (top). The averaged tilt angles of Ala6 and Val15 were 11.7° and 32.2°, respectively, which are in good agreement with those obtained by solid-state NMR experiments.

The rotational movements of the peptide around the helical axes were also investigated. Time courses for the phase angle (γ) of the peptide plane were measured for Ala6 and Val15 residues, and the results are shown in Fig. 9 (bottom). The angles changed from the initial value to the newly equilibrated values after approximately 30 ns. The averaged values of γ with respect to Ala6 and Val15 in the last 10 ns of the simulations were 82.7° (equivalent to −97.3°) and 56.6°, which are also very similar to those obtained by solid-state NMR experiments. However, it should be noted that the alamethicin peptide concentration in the NMR experiment was much higher than that used in the model for the MD simulation. In this simulation, we investigated the behavior of a single alamethicin peptide in membrane as a basic model. Nevertheless, it is noteworthy that the behavior of the single chain dynamics corresponds well with the experimental results.

The secondary structure of alamethicin in a lipid bilayer was investigated by analysis of the backbone dihedral angles of phi (C_n(C═O)–N_{n+1}–Cα_{n+1}–C_{n+1}(C═O)) and psi (N_n–Cα_n–C_n(C═O)–N_{n+1}). Table 3 shows the average dihedral angles of phi and psi between the neighboring residues of the alamethicin peptide in a DMPC bilayer during the last 10 ns of the simulation. The average

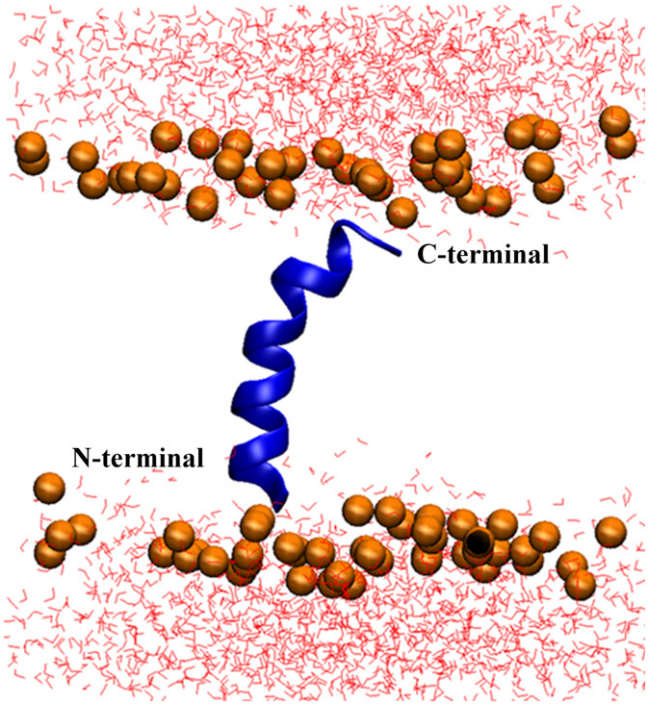

Fig. 8. Snapshot of alamethicin peptide in the DMPC membrane bilayer after simulation for 40 ns. Lipid phosphorus atoms and water molecules are shown with in orange and red, respectively. The side chain of alamethicin peptide and lipid atoms, and sodium and chloride ions are not shown for simplicity.

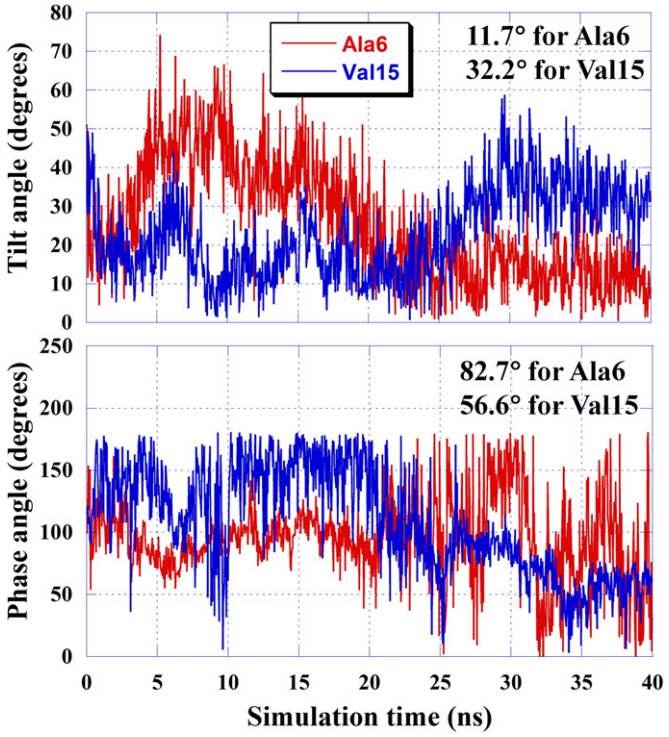

Fig. 9. Tilt angle ζ (top) and phase angle γ (bottom) for the carbonyl carbon atoms of the alamethicin peptide are shown as a function of the simulation time. The tilt angle ζ is calculated between the direction of the carbonyl group of the peptide and the membrane bilayer normal. The phase angle γ of the N-terminus was calculated from opposite site (N-terminus view) of NMR (C-terminus view) experimental result which is the same as 82.7° − 180° = −97.3°. Average (top) tilt angles ζ and (bottom) phase angle γ of carbonyl carbon atoms in the alamethicin peptide calculated during the last 10 ns of the MD simulation.

Table 3
Average dihedral angles (degrees) of phi and psi between residues of alamethicin peptide in DMPC bilayer during the last 10 ns simulation.

	Residue numbers																	
	1–2	2–3	3–4	4–5	5–6	6–7	7–8	8–9	9–10	10–11	11–12	12–13	13–14	14–15	15–16	16–17	17–18	18–19	19–20
Phi	−70.7	−61.8	−64.9	−52.7	−65.5	−59.2	−56.4	−66.6	−54.0	−73.9	−78.3	**−45.9**	−75.5	−84.1	**−52.4**	−58.2	−77.3	−77.2	−90.4
Psi		−27.7	−53.1	−44.7	−49.7	−44.1	−50.0	−45.7	−51.9	−42.0	**−38.3**	−45.8	−58.0	**−12.7**	−53.1	−52.0	**−33.4**	−41.7	−48.3

Bold: 3_{10}-helical values.

dihedral angles between residues of Gly11 and Aib13, Pro14 and Aib16, and Aib17 and Gln18 at the C-terminal side were the same as those for the 3_{10}-helix. On the other hand, the average dihedral angles between neighboring residues at the N-terminal side were the same as those for the α-helix. Thus, these results are also in good agreement with the solid-state NMR results.

The distances between carbonyl carbon and amide nitrogen atoms in the helical backbone for some selected residues, which are labeled 1-^{13}C and ^{15}N atoms in the REDOR solid-state NMR, were also calculated. Table 2 shows the distances between these two atoms that were averaged during the last 10 ns of the simulation, which. again shows that the calculated results are in good agreement with the experimental results.

4. Conclusion

The structure and orientation of alamethicin bound to a membrane were determined using the chemical shift oscillation of ^{13}C chemical shift anisotropy for individual ^{13}C labeled amino acid residues inserted in a transmembrane with the N- and C-termini forming α- and 3_{10}-helices, and the axes of the N- and C-termini were tilted 17° and 32° to the bilayer normal, respectively. The topology of the two helical axes was further determined using the internuclear distances around the bending region obtained from REDOR experiments, and energy minimization using the orientation of the N- and C-terminal helices and internuclear distances as constraints for topology analysis, which revealed that the alamethicin peptide takes a bending angle of 165° in the membrane environment. The dynamic behavior of alamethicin in membrane environments was further revealed by MD simulation and the calculation results showed that alamethicin establishes the bent structure after 40 ns. The N-terminal helix forms an α-helix with a tilt angle of 11° to the bilayer normal and the C-terminal helix forms a distorted 3_{10}-helix with a tilt angle of 32° to the bilayer normal, and the bending angle is 159°. These values are in good agreement with the experimentally determined values.

Conflict of interest

We do not have any conflict of interests.

Acknowledgment

This work was supported by Grants-in-Aid for Scientific Research on an Innovative area (26102514 and 26104513), and Grants-in-Aid for Scientific Research (C) (15K06963) and (B) (15H04336) from the Ministry of Education, Culture, Sports, Science and Technology of Japan.

We thank the Research Center for Computational Science, Okazaki, Japan for access to computing resources that executed part of the calculation.

Appendix A. Supplementary data

Supplementary data to this article can be found online at http://dx.doi.org/10.1016/j.bbamem.2015.07.019.

References

[1] C.E. Meyer, F. Reusser, A polypeptide antibacterial agent isolated from *Trichoderma viride*, Experientia 23 (1967) 85–86.
[2] R.C. Pandey, J.C. Cook Jr., K.L. Rinehart Jr., High resolution and field desorption mass spectrometry studies and revised structures of alamethicins I and II, J. Am. Chem. Soc. 99 (1977) 8469–8483.
[3] T.M. Balasubramanian, N.C.E. Kendrick, M. Taylor, G.R. Marshall, J.E. Hall, I. Vodyanoy, F. Reusser, Synthesis and characterization of the major component of alamethicin, J. Am. Chem. Soc. 103 (1981) 6127–6132.
[4] B. Leitgeb, A. Szekeres, L. Manczinger, C. Vágvölglyi, L. Kredics, The history of alamethicin: a review of the most extensively studied peptaibol, Chem. Biodivers. 4 (2007) 1027–1051.
[5] P. Mueller, D.O. Rudin, Action potentials induced in biomolecular lipid membranes, Nature 217 (1968) 713–719.
[6] K.H. Steve, J. Ludtke, W.T. Heller, H.W. Huang, Mechanism of alamethicin insertion into lipid bilayers, Biophys. J. 71 (1996) 2669–2679.
[7] P.C. Dave, E. Billington, Y.-L. Pan, S.K. Straus, Interaction of alamethicin with ether-linked phospholipid bilayers: Oriented circular dichroism, ^{31}P solid-state NMR, and differential scanning calorimetry studies, Biophys. J. 89 (2005) 2434–2442.
[8] D.P. Tieleman, H.J.C. Berendsen, M.S.P. Sansom, Voltage-dependent insesion of alamethicin of phospholipid/water and octan/water interface, Biophys. J. 80 (2001) 331–346.
[9] R.O. Fox Jr., F.M. Richards, A voltage-gated ion channel model inferred from the crystal structure of alamethicin at 1.5-Å resolution, Nature 300 (1982) 325–330.
[10] K.H. Steve, J. Ludtke, D.L. Worcester, H.W. Huang, Neutron scattering in the plane of membranes: structure of alamethicin pores, Biophys. J. 70 (1996) 2659–2666.
[11] J. Pan, S. Tristram-Nagle, J.F. Nagle, Alamethicin aggregation in lipid membranes, J. Membr. Biol. 231 (2009) 11–27.
[12] G.A. Woolley, B.A. Wallace, Model ion channels: gramicidin and alamethicin, J. Membr. Biol. 129 (1992) 109–136.
[13] M.S.P. Sansom, Alamethicin and related peptaibols — model ion channels, Eur. Biophys. J. 22 (1993) 105–124.
[14] U. Banerjee, F.-P. Tsui, T.N. Balasubramanian, G.R. Marshall, S.I. Chan, Structure of alamethicin in solution: one- and two-dimensional ^{1}H nuclear magnetic resonance studies at 500 MHz, J. Mol. Biol. 165 (1983) 757–775.
[15] G. Esposito, J.A. Carver, J. Boyd, I.D. Campbell, High-resolution ^{1}H NMR study of the solution structure of alamethicin, Biochemistry 26 (1987) 1043–1050.
[16] A.A. Yee, J.D.J. O'Neil, Uniform ^{15}N labeling of a fungal peptide: the structure and dynamics of an alamethicin by ^{15}N and ^{1}H NMR spectroscopy, Biochemistry 31 (1992) 3135–3143.
[17] J.C. Franklin, J.F. Ellena, S. Jayasinghe, L.P. Kelsh, D.S. Cafiso, Structure of micelle-associated alamethicin from ^{1}H NMR. Evidence for conformational heterogeneity in a voltage-gated peptide, Biochemistry 33 (1994) 4036–4045.
[18] G. Jung, N. Dubischar, D. Leibfritz, Conformational changes of alamethicin induced by solvent and temperature. A ^{13}C–NMR and circular-dichroism study, Eur. J. Biochem. 54 (1975) 395–409.
[19] A.P. New, C. Eckers, N.J. Haskins, W.A. Neville, S. Elson, J.A. Hueso-Rodrfguez, A. Rivera-Sagredo, Structures of polysporins A–D, four new peptaibols isolated from *trichoderma polysporum*, Tetrahedron Lett. 37 (1996) 3039–3042.
[20] A. Psurek, C. Neusüβ, M. Pelzing, G.K.E. Scriba, Analysis of the lipophilic peptaibol alamethicin by nonaqueous capillary electrophoresis–electrospray ionization-mass spectrometry, Electrophoresis 26 (2005) 4368–4378.
[21] A. Psurek, C. Neusüβ, T. Degenkolb, H. Brückner, E. Balaguer, D. Imhof, G.K.E. Scriba, Detection of new amino acid sequences of alamethicins F30 by nonaqueous capillary electrophoresis-mass spectrometry, J. Pept. Sci. 12 (2006) 279–290.
[22] H. Saitô, R. Tabeta, F. Formaggio, M. Crisma, C. Toniolo, High-resolution solid-state ^{13}C–NMR of peptides: A study of chain-length dependence for 3_{10}-helix formation, Biopolymers 27 (1988) 1607–1617.
[23] T. Nagao, A. Naito, S. Tuzi, H. Saitô, Conformation and orientation of biologically active peptide alamethicin in phospholipid bilayer by high-resolution solid-state NMR spectroscopy, Pept. Sci. (1998) 341–344.
[24] C.L. North, M. Barranger-Mathys, D.S. Cafiso, Membrane orientation of the N-terminal segment of alamethicin determined by solid-state ^{15}N NMR, Biophys. J. 69 (1995) 2392–2397.
[25] M. Bak, R.P. Bywater, M. Hohwy, J.K. Thomsen, K. Adelhorst, H.J. Jakobsen, O.W. Sørensen, N.C. Nielsen, Conformation of alamethicin in oriented phospholipid bilayers determined by ^{15}N solid-state nuclear magnetic resonance, Biophys. J. 81 (2001) 1684–1698.
[26] K. Bertelsen, B. Paaske, L. Thøgersen, E. Tajkhorshid, B. Schiøtt, T. Skrydstrup, N.C. Nielsen, T. Vosegaard, Residue-specific information about the dynamics of antimicrobial peptides from ^{1}H–^{15}N and ^{2}H solid-state NMR spectroscopy, J. Am. Chem. Soc. 131 (2009) 18335–18342.

[27] B. Bechinger, D.A. Skladnev, A. Ogrel, X. Li, E.V. Rogozhkina, T.V. Ovchinnikova, J.D.J. O'Neil, J. Raap, ^{15}N and^{31}P solid-state NMR investigation on the orientation of zervamicin II and alamethicin in phosphatidylcholine membranes, Biochemistry 40 (2001) 9428–9437.
[28] E.S. Sainikov, H. Friedrich, X. Li, P. Bertani, S. Reissmann, C. Hertweck, J.D.J. O'Neil, J. Raap, B. Bechinger, Structure and alignment of the membrane-associated peptaibols ampullosporin A and alamethicin by oriented ^{15}N and ^{31}P solid-state NMR spectroscopy, Biophys. J. 96 (2009) 86–100.
[29] A. Naito, Structure elucidation of membrane-associated peptides and proteins in oriented bilayers by solid-state NMR spectroscopy, Solid State Nucl. Magn. Reson. 36 (2009) 67–76.
[30] A. Naito, T. Nagao, K. Norisada, T. Mizuno, S. Tuzi, H. Saitô, Conformation and dynamics of melittin bound to magnetically oriented lipid bilayers by solid-state ^{31}P and^{13}C NMR spectroscopy, Biophys. J. 78 (2000) 2405–2417.
[31] S. Toraya, K. Nishimura, A. Naito, Dynamic structure of vesicle-bound melittin in a variety of lipid chain length by solid-state NMR, Biophys. J. 87 (2004) 3323–3335.
[32] T. Uezono, S. Toraya, M. Obata, K. Nishimura, S. Tuzi, H. Saitô, A. Naito, Structure and orientation of dynorphin bound to lipid bilayers by ^{13}C solid-state NMR, J. Mol. Struct. 749 (2005) 13–19.
[33] S. Toraya, N. Javkhlantugs, D. Mishima, K. Nishimura, K. Ueda, A. Naito, Dynamic structure of bombolitin II bound to lipid bilayer as revealed by solid-state NMR and molecular-dynamics simulation, Biophys. J. 99 (2010) 3282–3289.
[34] A. Tsutsumi, N. Javkhlantugs, A. Kira, M. Umeyama, I. Kawamura, K. Nishimura, K. Ueda, A. Naito, Structure and orientation of bovine lactoferrampin in the mimetic bacterial membrane as revealed by solid-state NMR and molecular dynamics simulation, Biophys. J. 103 (2012) 1735–1743.
[35] N. Javkhlantugs, A. Naito, K. Ueda, Molecular dynamics simulation of Bombolitin II in the dipalmitoylohosphatidylcholine membrane bilayer, Biophys. J. 101 (2011) 1212–1220.
[36] Y. Wang, D.E. Schlamadinger, J.E. Kim, J.A. McCammon, Comparative molecular dynamics simulation of the antimicrobial peptide CM15 in model lipid bilayers, Biochim. Biophys. Acta 1818 (2012) 1402–1409.
[37] S. Promsri, G.M. Ullmann, S. Hannongbua, Molecular dynamics simulation of HIV-1 fusion domain-membrane complexes: Insight into the N-terminal gp41 fusion mechanism, Byophys. Chem. 170 (2012) 9–16.
[38] M.H. Khatami, M. Bromberek, I. Saika-Voivod, V. Booth, Molecular dynamics simulation of histidine-containing cod antimicrobial peptide paralogs in self-assembled bilayers, Biochim. Biophys. Acta 1838 (2014) 2778–2787.
[39] A. Kira, N. Javkhlantugs, T. Miyamori, Y. Sasaki, M. Eguchi, I. Kawamura, K. Ueda, A. Naito, Interaction of extracellular loop II of k-opioid receptor (196–228) with opioid peptide dynorphin in membrane environments as revealed by solid state nuclear magnetic resonance, quartz crystal microbalance and molecular dynamics simulation, J. Phys. Chem. B 118 (2014) 9604–9612.
[40] A. Paquet, Introduction of 9-fluorenylmethyloxycarbonyl, trichloroethoxycarbonyl, and benzyloxycarbonyl amine protecting groups into O-unprotected hydroxyamino acids using succinimidyl carbonates, Can. J. Chem. 60 (1982) 976–980.
[41] W.C. Chan, P.D. White, Basic procedure, Fmoc solid phase peptide synthesis, in: W.C. Chan, P.D. White (Eds.), Oxford Univ. Press 2000, pp. 41–76.
[42] T. Gullion, J. Schaefer, Elimination of resonance offset effects in rotational-echo double-resonance NMR, J. Magn. Reson. 92 (1991) 439–442.
[43] A. Naito, K. Nishimura, S. Kimura, S. Tuzi, M. Aida, N. Yasuoka, H. Saitô, Determination of the three-dimensional structure of a new crystalline form of *N*-acetyl-Pro-Gly-Phe as revealed by ^{13}C REDOR, X-ray diffraction, and molecular dynamics calculation, J. Phys. Chem. 100 (1996) 14995–15004.
[44] B.R. Brooks, R.E. Bruccoleri, B.D. Olafson, D.J. States, S. Swaminathan, M. Karplus, CHARMM: A program for macromolecular energy, minimization, and dynamics calculations, J. Comput. Chem. 4 (1983) 187–217.
[45] A.D. Mackerell Jr., D. Bashford, M. Bellott, R.L. Dunbrack Jr., J.D. Evanseck, M.J. Field, S. Fischer, J. Gao, H. Guo, S. Ha, D. Joseph-McCarthy, L. Kuchnir, K. Kuczera, F.T.K. Lau, C. Mattos, S. Michnick, T. Ngo, D.T. Nguyen, B. Prodhom, W.E. Reiher III, B. Roux, M. Schlenkrich, J.C. Smith, R. Stote, J. Straub, M. Watanabe, J. Wiórkiewicz-Kuczera, D. Yin, M. Karplus, All-atom empirical potential for molecular modeling and dynamics studies of proteins, J. Phys. Chem. B 102 (1998) 3586–3616.
[46] J.B. Klauda, R.M. Venable, J.A. Freites, J.W. O'Connor, D.J. Tobias, C. Mondragon-Ramirez, I. Vorobyov, A.D. MacKerell Jr., R.W. Pastor, Updata of the CHARMM all-atom additive force field for lipids: Validation on six lipid types, J. Phys. Chem. B 114 (2010) 7830–7843.
[47] S. Jo, T. Kim, W. Im, Automated builder and database of protein/membrane complexes for molecular dynamics simulations, PloS One 2 (2007) e880.
[48] S. Jo, T. Kim, V.G. Iyer, W. Im, CHARMM-GUI: a web-based graphical user interface for CHARMM, J. Comput. Chem. 29 (2008) 1859–1865.
[49] H. Saitô, I. Ando, High-resolution solid-state NMR studies of synthetic and biological macromolecules, Annu. Rep. NMR Spectrosc. 21 (1989) 209–290.
[50] H. Saitô, I. Ando, A. Ramamoorthy, Chemical shift tensor — the heart of NMR: insights into biological aspect of proteins, Prog. Nucl. Magn. Reson. Spectrosc. 57 (2010) 181–228.
[51] J. Dittmer, L. Thøgersen, J. Underhaug, K. Bertelsen, T. Vosegaard, J.M. Pedersen, B. Schiøtt, E. Tajkhorshid, T. Skrydstrup, N.C. Nielsen, Incorporation of antimicrobial peptides into membranes: a combined liquid-state NMR and molecular dynamics study of alamethicin in DMPC/DHPC bicelles, J. Phys. Chem. B 113 (2009) 6928–6937.